

# Influence of sintering additives on indentation cracks and deformation in silicon nitride

E. Gondár<sup>1\*</sup>, Z. Gábrišová<sup>1</sup>, M. Roško<sup>1</sup>, M. Zemánková<sup>2</sup>

<sup>1</sup>*Faculty of Mechanical Engineering, Slovak University of Technology Bratislava, Pionierska 15, 812 31 Bratislava, Slovak Republic*

<sup>2</sup>*Institute of Materials and Machine Mechanics, Slovak Academy of Sciences, Račianska 75, 831 02 Bratislava, Slovak Republic*

Received 27 October 2005, received in revised form 20 March 2006, accepted 23 March 2006

## Abstract

The depth profile of indented cracks in silicon nitride with MgO additive was determined by serial sectioning and observation of fracture areas. These cracks were of Palmqvist's type, in contrary to the  $\text{Si}_3\text{N}_4$  with  $\text{Al}_2\text{O}_3 + \text{Y}_2\text{O}_3$  additives. A deformed/damaged zone was identified under the indent with a depth ranging from 420 to 490  $\mu\text{m}$ . The volume of the indent represents on average 5 % of the volume of the deformed zone. The deformed zone of silicon nitride with MgO additive was approximately 3 times higher than in the silicon nitride sintered with additives of  $\text{Al}_2\text{O}_3 + \text{Y}_2\text{O}_3$ . The shape of the deformed zone was angular for both materials, although their character is different. In the case of specimens with  $\text{Al}_2\text{O}_3 + \text{Y}_2\text{O}_3$  additives, the fracture area circumvents the deformed zone, whereas in the case of MgO additive the fracture passes through it. The number of minor cracks, initiated during indentation with Vickers indenter was lower in the case of silicon nitride with MgO additive, which renders the value of fracture toughness more reliable for this material.

**Key words:** silicon nitride, deformation under indent, depth profile of cracks, serial sectioning, fracture area

## 1. Introduction

Silicon nitride, with its outstanding properties like high hardness, abrasion resistance, chemical stability, creep resistance and high-temperature strength up to 1400 °C, is especially suitable for high-temperature applications [1, 2]. The high-temperature mechanical properties and oxidation resistance of  $\text{Si}_3\text{N}_4$  depend to a great extent on the character of the secondary phase, i.e. on the sintering additives used during production of the material [3]. The maximum application temperature, for example, is 1350 °C in the case of sintering additives  $\text{Al}_2\text{O}_3 + \text{Y}_2\text{O}_3$ , whereas it is only 1000 °C in the case of MgO.

High-temperature applications require a development of appropriate testing methods to determine the resistance of ceramic parts. These materials often have to withstand thermal shocks. On the Department of Materials and Technologies of the Faculty of Mecha-

anical Engineering of the Slovak University of Technology, a new testing method has been developed [4] and optimized [5] to test the resistance of technical ceramics to repeated thermal shocks. The testing method is protected by a patent [6]. Until now,  $\text{Si}_3\text{N}_4$  specimens with sintering additives  $\text{Al}_2\text{O}_3 + \text{Y}_2\text{O}_3$  have been used in the test [7]. Along with the new testing method, a computer simulation has been developed [8] and verified [9], which simulates the temperature and stress conditions in the specimen subjected to repeated thermal shocks. For this simulation it is necessary to know the depth profile of cracks initiated in the specimen before the test using Vickers indenter. The determination of the depth profile has been described in several studies so far [10–12]. The subject of this article is the study of depth profile of cracks, initiated in silicon nitride with MgO additive and comparison of this profile with the one studied in silicon nitride with  $\text{Al}_2\text{O}_3 + \text{Y}_2\text{O}_3$  additives in [12]. The depth profile is

\*Corresponding author: tel.: 02/44455087-367; fax: 02/44455086; e-mail address: ernest.gondar@stuba.sk

necessary for determination of critical stress needed for an unstable crack growth [9] during the loading of the specimen.

## 2. Experimental materials and methods

The experimental material was prepared by cold pressing and then hot pressing in nitrogen atmosphere. The hot pressing of the experimental material was performed on a laboratory hot press with a special construction of heating body [13], under the following conditions:  $T = 1750^\circ\text{C}$ ,  $p = 30\text{ MPa}$ ,  $t = 30\text{ min}$ .

Activating sintering additive of silicon nitride was magnesia MgO with mass ratio: 95 wt.%  $\text{Si}_3\text{N}_4$  + 5 wt.% MgO.

In this article, the experimental material will be compared with  $\text{Si}_3\text{N}_4$  with sintering additives  $\text{Al}_2\text{O}_3$  +  $\text{Y}_2\text{O}_3$ , studied in [12], which was prepared using the same device and parameters, with mass ratio 85.36 wt.%  $\text{Si}_3\text{N}_4$  + 10.34 wt.%  $\text{Y}_2\text{O}_3$  + 4.30 wt.%  $\text{Al}_2\text{O}_3$ .

The density of the specimens was determined by Archimedes method. Average porosity was 1.76 % with maximum value of 2.1 % and minimum value 1.6 %. Specimens with diameter of 8 mm and thickness of 2 mm were prepared and subsequently ground and polished on STRUERS PEDEMIN-S device. A total of twelve specimens were prepared for the study. In the middle of each specimen, cracks were initiated with Vickers indenter using HPO 250 device with the following parameters:

loading force  $F = 294.3\text{ N}$ , time  $t = 15\text{ s}$ ,  
room temperature  $T = 20^\circ\text{C}$ .

Five specimens were used for the observation of the depth profile. Two indents were made into each of these specimens, hence the total number of observed indents was 10. The other specimens were used for the examination of fracture areas.

The HV hardness was determined from the diagonals of the indent. From the dimension ratio of indent and cracks, the cracks were determined to be of Palmqvist's type. Subsequently, fracture toughness was calculated from the formula [14] for this type of cracks:

$$K_{\text{IC}} = 0.0889 \sqrt{\left(\frac{H \cdot P}{4l}\right)}, \quad (1)$$

where  $H$  is hardness [MPa],  $P$  is indentation force [N],  $l$  is average length of cracks [ $\mu\text{m}$ ].

Serial sectioning of the indented side of the specimen was performed using grinding discs with diamond paste. The sectioning took place in direction parallel with the surface of the specimen, contrary to [11], where the direction of sectioning was perpendicular to the surface. The thickness of removed layer  $H$  was determined from the geometry of the indent, where  $L1$

is the length of diagonal before sectioning [ $\mu\text{m}$ ],  $L2$  is the length of diagonal after sectioning [ $\mu\text{m}$ ],

$$H = \frac{L1 - L2}{\frac{2}{\text{tg} \frac{136^\circ}{2}}}. \quad (2)$$

After removing the indent, the depth reference would be lost. Because of this, new indent was created before removing the original one. This process was repeated throughout the whole sectioning. Only diagonals were measured on the new indents, as they served only as a depth reference.

## 3. Results and discussion

Schematic progress of serial sectioning is shown in Fig. 1, where Fig. 1a represents the depth profile of the cracks in vertical direction and Fig. 1b shows the shape of the impression, cracks and deformed zone during the sectioning. Unlike in  $\text{Si}_3\text{N}_4$  with  $\text{Al}_2\text{O}_3$  +  $\text{Y}_2\text{O}_3$  additives, the indented cracks in our experimental material are of Palmqvist's type.

Gradual change of the measured area can be described in 4 steps. Step 0 represents the original state

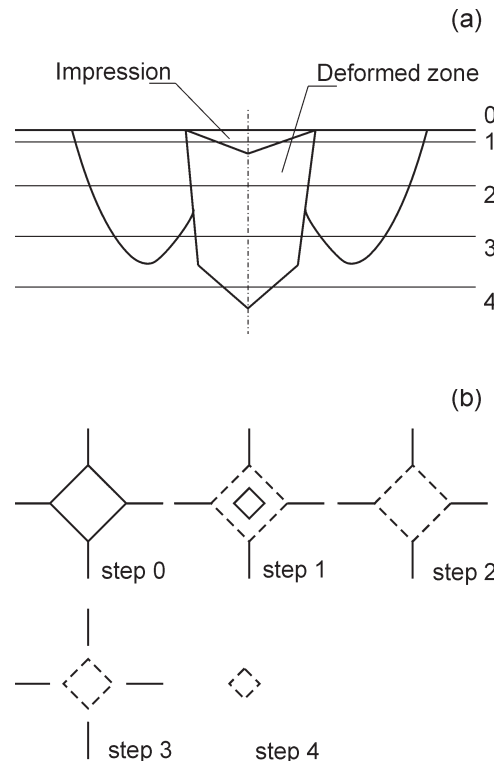


Fig. 1. Schematic progress of serial sectioning: a) depth profile, b) top view.

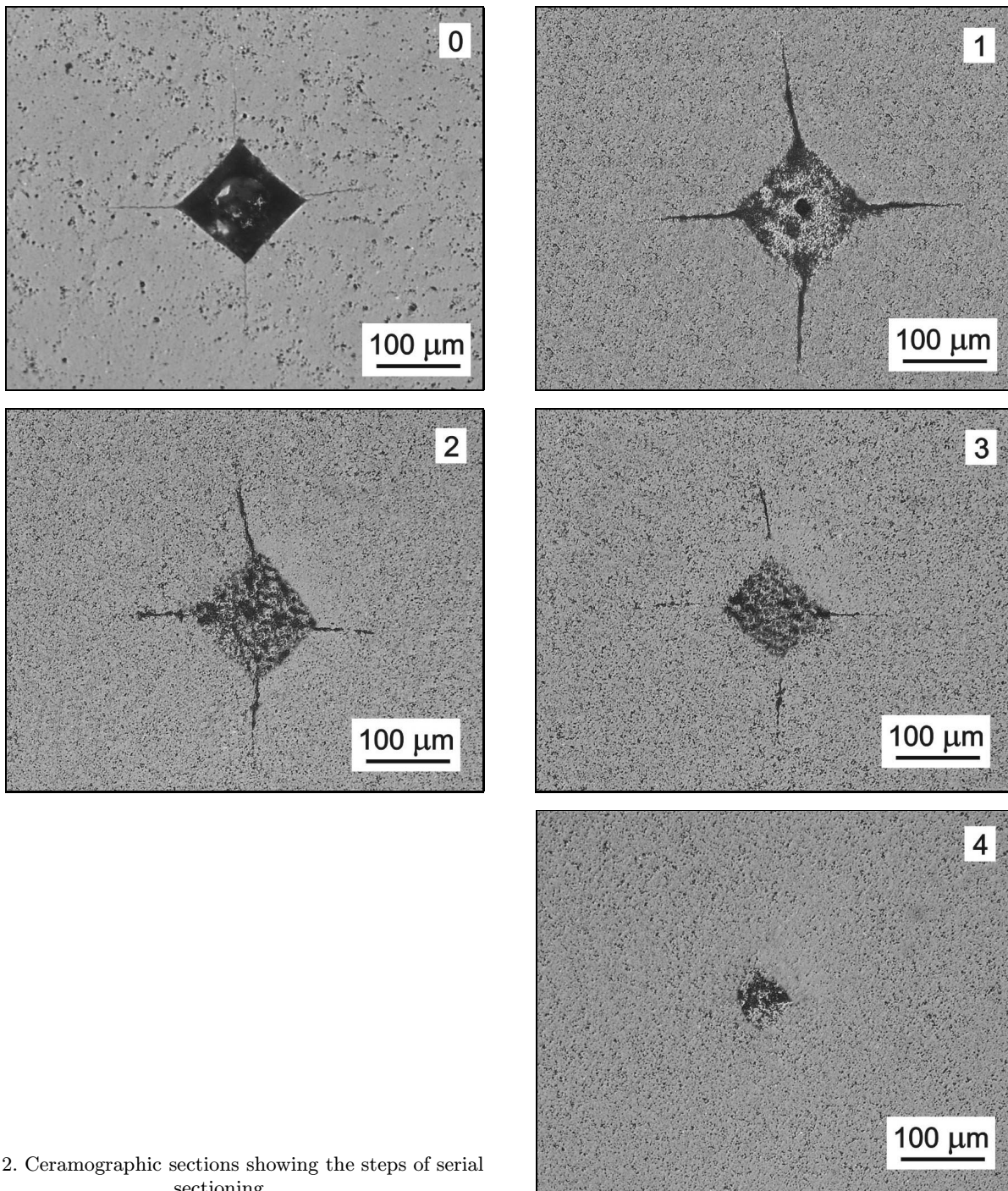


Fig. 2. Ceramographic sections showing the steps of serial sectioning.

before ablation. Step 1 represents a depth, in which the indent (bold line) has not yet been removed. The deformed zone is shown as dashed line. In steps 2 and 3, the indent is already removed. Step 3 represents a noticeable decrease in the size of the deformed zone. Step 4 corresponds to a depth, in which the cracks have been removed. The residual part of the deformed zone is again shown as dashed line. From Fig. 1 follows, that the initiated cracks are of Palmqvist's type, i.e. their depth is smaller than the depth of the deformed zone. Ceramographic sections, show-

ing the steps defined above, are shown in Fig. 2. After the first ablation, also minor cracks were identified, which originated at the edge of the deformed zone. Their depth was between  $145\ \mu\text{m}$  and  $175\ \mu\text{m}$ . The number of these minor cracks was considerably lower than the one stated in [12]. It can be assumed, that the amount and size of the minor cracks influences the determination of fracture toughness  $K_{IC}$ . The energy of indentation is not depleted only for the creation of deformed zone and major cracks, but also for the creation of minor cracks under the surface. These are not

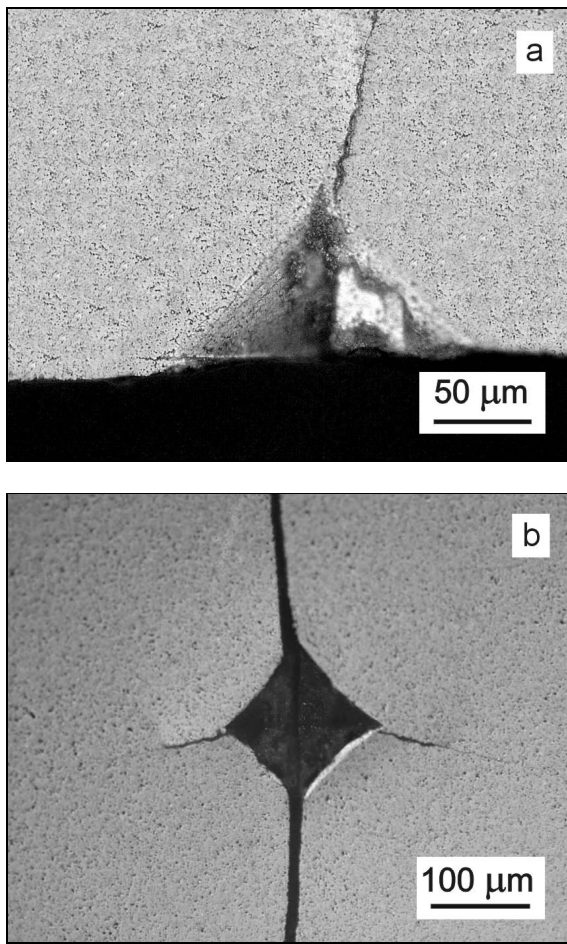


Fig. 3. Broken specimen: a) fracture straight through the indent and deformed zone, b) broken halves of the specimen put together.

taken into account when calculating fracture toughness. Since the amount of minor cracks is low in the case of silicon nitride with MgO additive, the calculated value of  $K_{IC} = 8.1 \text{ MPa} \cdot \text{m}^{1/2}$  can be assumed more reliable than the value of  $K_{IC} = 4.8 \text{ MPa} \cdot \text{m}^{1/2}$  calculated for  $\text{Si}_3\text{N}_4$  with  $\text{Al}_2\text{O}_3 + \text{Y}_2\text{O}_3$  additives.

The depth of deformed zone ranges from  $420 \mu\text{m}$  to  $490 \mu\text{m}$  (average value  $451.5 \mu\text{m}$ ), which is approximately 3 times bigger than the depth measured in [12]. We assume that the deformation under the indenter was less intense when compared to [12]. The fracture of the specimens took place straight through the deformed zone (Fig. 3), contrary to the material with  $\text{Al}_2\text{O}_3 + \text{Y}_2\text{O}_3$  additives, where the fracture circumvented the deformed zone. The assumption of lesser deformation intensity is supported also by lower amount of minor cracks. There are also no cracks located on the interface between the deformed and undeformed zone, as seen in [12]. From these facts it can be assumed that the intensity of volume changes in the deformed zone was lower, hence the stresses on the

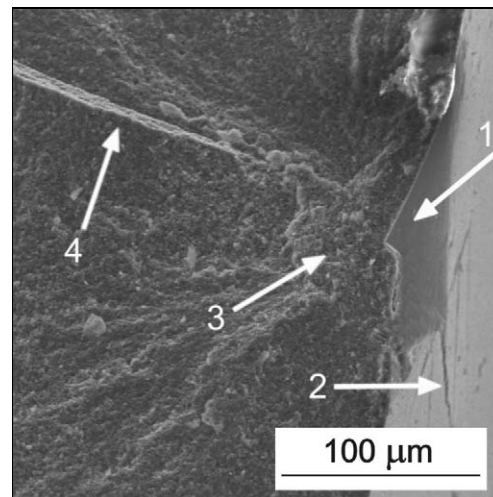


Fig. 4. Detail of the fracture area: 1 – half of the indent, 2 – crack, 3 – deformed zone, 4 – interface of bridging.

interface between the deformed and undeformed zone in specimens with MgO additive were lower as well.

Figure 4 shows a detail of the fracture area. Arrow 1 shows the remainder of the indent, arrow 2 shows the crack and arrow 3 points at the deformed zone. Neither defects nor cracks were identified within the deformed zone, as they were in the case of silicon nitride with  $\text{Al}_2\text{O}_3 + \text{Y}_2\text{O}_3$  additives. An indication of growth progress lines can be seen under the deformed zone, hence the fracture should not be considered as purely brittle. Arrow 4 points at a bridging of the fracture area from the lower to the upper part of the fracture.

Graphical representation of the measured values and the resulting depth profile of cracks and deformed zone are shown in Fig. 5. The cracks are not symmetrical to each other with respect to the deformed zone.

The depth of the deformed zone can be according to [15] calculated from the formula:

$$h \approx (p/H)^{1/2} \cdot (E/H)^{2/5}, \quad (3)$$

where  $p$  is indentation load [N] (294 N),  $E$  is Young's modulus of elasticity [MPa] (310 GPa),  $H$  is Vickers hardness [MPa] (14289.86 MPa).

The value of hardness is a mean value from 10 measurements, with the smallest value being 14065.46 MPa and the highest being 14597.86 MPa. The depth of the deformed zone, calculated from (3), is  $491 \mu\text{m}$ . Average depth measured during the experiments is  $451.5 \mu\text{m}$ . Maximum measured depth was  $490 \mu\text{m}$ , minimum value was  $420 \mu\text{m}$ . From the results follows, that the formula (3) can be accepted, which is contrary to the results for  $\text{Si}_3\text{N}_4$  with  $\text{Al}_2\text{O}_3 + \text{Y}_2\text{O}_3$  additives [12].

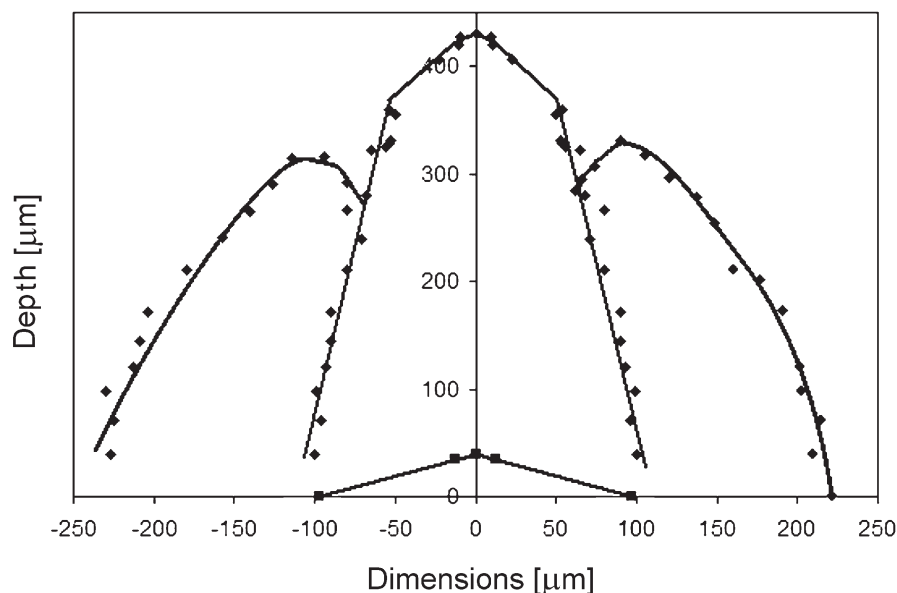


Fig. 5. Depth profile of cracks and deformed zone.

Next step in the study of the deformed area was to compare its volume with the volume of the indent. The aim of this comparison is to obtain an idea about the creation of the deformed zone. The deformed zone has a shape of truncated pyramid, almost a brick-like shape. This shape is similar to the one of  $\text{Si}_3\text{N}_4$  with  $\text{Al}_2\text{O}_3 + \text{Y}_2\text{O}_3$  additives, the only difference being the size. The bottom part of the deformed zone was less angular, with rounded ending. Different shape and size of the deformed zone, as well as different depth profile of the cracks, indicate a different location of crack initiation and propagation during indentation loading in  $\text{Si}_3\text{N}_4$  with  $\text{Al}_2\text{O}_3 + \text{Y}_2\text{O}_3$  and  $\text{MgO}$ . The crack in  $\text{Si}_3\text{N}_4$  with  $\text{Al}_2\text{O}_3 + \text{Y}_2\text{O}_3$  was probably initiated on the tip of the deformed zone and propagated to the surface, creating thus a half-penny shape of a central crack. This mechanism, described in [16], could have caused extensive stresses at the interface between deformed and undeformed zone. The shape of the deformed zone also supports the theory of this mechanism. Besides, a sharp tip at the bottom of the deformed zone, which was not assumed in [16], acted as a stress concentrator. Lower stresses at the interface between deformed and undeformed zone in  $\text{Si}_3\text{N}_4$  with  $\text{MgO}$  probably caused the crack initiation at the edges of the indenter or of the deformed zone, which were acting as preferential stress concentrators.

The volume of these bodies was calculated using basic geometric formulae. Subsequently, this volume was compared with the volume of the indents. The volume of the indent represents on average 5.15 % of the volume of the deformed area, taking into account the mean values from 10 indents (with maximum deviation of 14.35 %). Maximum value was 4.5 %, minimum value was 5.7 %.

The porosity of the specimens (1.6–2.1 %) represents approximately one third of the calculated ratio, hence this part of the deformed zone under the indent could have been created by filling the pores. We assume, that the remaining two thirds were deformed by filling defective regions in the binding phase during indentation. This mechanism was not as intense as in the case of silicon nitride with  $\text{Al}_2\text{O}_3$  and  $\text{Y}_2\text{O}_3$  additives [12]. The reason for this is a more compact binding phase with  $\text{MgO}$ . Lesser volume changes by creation of deformed zone cause in fact a lower number of defects in this zone when compared to silicon nitride with  $\text{Al}_2\text{O}_3$  and  $\text{Y}_2\text{O}_3$  additives.

#### 4. Conclusions

The achieved results can be summarized as follows:

- Sintering additives  $\text{Al}_2\text{O}_3 + \text{Y}_2\text{O}_3$  and  $\text{MgO}$  have a decisive influence on the crack initiation and propagation during indentation with Vickers indenter.
- Indentation cracks in  $\text{Si}_3\text{N}_4$  with  $\text{MgO}$  additive are of Palmqvist's type, unlike those in  $\text{Si}_3\text{N}_4$  with  $\text{Al}_2\text{O}_3 + \text{Y}_2\text{O}_3$  additives, which are of half-penny shape.
- The shape of the deformed/damaged zone in both investigated materials under the indent is angular, with a sharp pyramidal tip.
- Depth of the deformed zone in the  $\text{Si}_3\text{N}_4$  with  $\text{MgO}$  ranges from 420  $\mu\text{m}$  to 490  $\mu\text{m}$ , which is in good agreement with the calculated value of 491.13  $\mu\text{m}$ . This depth is approximately 3 times greater in comparison to the depth in  $\text{Si}_3\text{N}_4 + \text{Al}_2\text{O}_3 + \text{Y}_2\text{O}_3$ .
- Intensity of the volume changes in the deformed

zone of  $\text{Si}_3\text{N}_4 + \text{MgO}$  is lower than in  $\text{Si}_3\text{N}_4 + \text{Al}_2\text{O}_3 + \text{Y}_2\text{O}_3$  and the deformed zones are without noticeable defects.

The reliability of calculated value of  $K_{IC} = 8.1 \text{ MPa}\cdot\text{m}^{1/2}$  for  $\text{Si}_3\text{N}_4 + \text{MgO}$  is supported by a considerably lower amount of minor cracks than in the case of silicon nitride with  $\text{Al}_2\text{O}_3 + \text{Y}_2\text{O}_3$  additives.

### References

- [1] PÁNEK, Z.—FIGUSCH, V.—HAVIAR, M.—LIČKO, T.—ŠAJGALÍK, P.—DUSZA, J.: Konštrukčná keramika. Bratislava, R&D 1992.
- [2] HVIZDOŠ, P.—KAŠIAROVÁ, M.—HNATKO, M.—ŠAJGALÍK, P.: Kovove Mater., 42, 2004, p. 51.
- [3] KOVALČÍK, J.—HVIZDOŠ, P.—DUSZA, J.—ŠAJGALÍK, P.—HNATKO, M.—REECE, M.: Kovove Mater., 41, 2003, p. 377.
- [4] GONDÁR, E.—PULC, V.—KRIŽANSKÁ, M.: In: Technológia '95. STU Bratislava 1995, p. 34, ISBN 80-227-0782-1.
- [5] GONDÁR, E.: The testing method of resistance of silicon nitride based technical ceramics to thermal loading, Conferment project, Sjf STU Bratislava 1998.
- [6] GONDÁR, E.—PULC, V.—ŠVEC, P.: Spôsob skúšania keramiky na odolnosť proti tepelnej únave. AO č. 284 53, 1.7.2005, Vestník ÚPV SR č. 7/2005.
- [7] GONDÁR, E.—PULC, V.—BABJAKOVÁ, Z.: Pokroky práškovej metalurgie, 36, 1998, p. 44.
- [8] BERKY, B.—GONDÁR, E.—PULC, V.: In: Zborník z medzinárodnej konferencie pri príležitosti 45. výročia založenia Strojníckej fakulty TU v Košiciach. TU Košice 1997, p. 7.
- [9] GONDÁR, E.—HLAVA, T.—ROŠKO, M.: J. Eur. Ceram. Soc., 2005 (in press).
- [10] DUSZA, J.: Scripta Met. et Mat., 26, 1992, p. 337.
- [11] LUBE, T.: J. Eur. Ceram. Soc., 21, 2001, p. 211.
- [12] GONDÁR, E.—ROŠKO, M.—ZEMÁNKOVÁ, M.: Kovove Mater., 43, 2005, p. 124.
- [13] PULC, V.—GONDÁR, E.—ŠVEC, P.: In: Zborník z medzinárodnej konferencie pri príležitosti 40. výročia založenia Strojníckej fakulty TU v Košiciach. TU Košice 1992, p. 97.
- [14] SHETTY, D. K.—WRIGHT, I. G.—MINCER, P. N.—CLAUER, A. H.: J. Mater. Sci., 20, 1985, p. 1873.
- [15] EVANS, A. G.—WILSHAW, T. R.: Acta Metallurgica, 24, 1976, p. 939.
- [16] FETT, T.—KOUNGA NJIWA, A. B.—RÖDEL, J.: Engineering Fracture Mechanics, 72, 2005, p. 647.